bioRxiv preprint doi: https://doi.org/10.1101/697318; this version posted July 19, 2019. The copyright holder for this preprint (which was not certified by peer review) is the author/funder, who has granted bioRxiv a license to display the preprint in perpetuity. It is made available under aCC-BY-NC-ND 4.0 International license.

Genome Biology

(submitted)

Power and pitfalls of computational methods for inferring clone phylogenies and mutation orders from bulk sequencing data

Sayaka Miura[1,2], Tracy Vu[1,2], Jiamin Deng[1,2], Tiffany Buturla[1,2], Jiyeong Choi[1,2], and Sudhir Kumar[1,2,3*]

[1]Institute for Genomics and Evolutionary Medicine, [2]Department of Biology, Temple University, Philadelphia, PA 19122, USA.[3]Center for Excellence in Genome Medicine and Research, King Abdulaziz University, Saudi Arabia.

SM: tuf78332@templ.edu
TV: tug86468@temple.edu
JD: tug64096@temple.edu
TB: tug42548@temple.edu
JC: tuh48344@temple.edu

Correspondence to:
Sudhir Kumar
Temple University
Philadelphia, PA 19122, USA
E-mail: s.kumar@temple.edu

bioRxiv preprint doi: https://doi.org/10.1101/697318; this version posted July 19, 2019. The copyright holder for this preprint (which was not certified by peer review) is the author/funder, who has granted bioRxiv a license to display the preprint in perpetuity. It is made available under aCC-BY-NC-ND 4.0 International license.

Abstract

Background. Tumors harbor extensive genetic heterogeneity in the form of distinct clone genotypes that arise over time and across different tissues and regions of a cancer patient. Many computational methods produce clone phylogenies from population bulk sequencing data collected from multiple tumor samples. These clone phylogenies are used to infer mutation order and clone origin times during tumor progression, rendering the selection of the appropriate clonal deconvolution method quite critical. Surprisingly, absolute and relative accuracies of these methods in correctly inferring clone phylogenies have not been consistently assessed.

Methods. We evaluated the performance of seven computational methods in producing clone phylogenies for simulated datasets in which clones were sampled from multiple sectors of a primary tumor (multi-region) or primary and metastatic tumors in a patient (multi-site). We assessed the accuracy of tested methods metrics in determining the order of mutations and the branching pattern within the reconstructed clone phylogenies.

Results. The accuracy of the reconstructed mutation order varied extensively among methods (9% – 44% error). Methods also varied significantly in reconstructing the topologies of clone phylogenies, as 24% – 58% of the inferred clone groupings were incorrect. All the tested methods showed limited ability to identify ancestral clone sequences present in tumor samples correctly. The occurrence of multiple seeding events among tumor sites during metastatic tumor evolution hindered deconvolution of clones for all tested methods.

Conclusions. Overall, CloneFinder, MACHINA, and LICHeE showed the highest overall accuracy, but none of the methods performed well for all simulated datasets and conditions.

Keywords: Clone phylogeny; bulk sequencing; tumor evolution; mutation order

bioRxiv preprint doi: https://doi.org/10.1101/697318; this version posted July 19, 2019. The copyright holder for this preprint (which was not certified by peer review) is the author/funder, who has granted bioRxiv a license to display the preprint in perpetuity. It is made available under aCC-BY-NC-ND 4.0 International license.

Background

Somatic mutations play a crucial role in cancer progression [1-3]. Early models proposed that clones with driver mutations sweep through the population, which is called a linear progression of clone evolution [4]. Now, it is clear that tumors are not monoclonal, and that the clonal evolution generally follows a branching model (i.e., incomplete clonal sweep) even within a tumor [4-10]. Similarly, metastatic tumors also follow a branching pattern [11, 12]. Clones found in primary and metastatic tumors show inter- and intra-tumor evolutionary relationships, which can be represented by a single-patient clone phylogeny [13-16] (e.g., **Fig. 1g and 1h**). The reconstruction and analysis of clone phylogenies have become standard practices in cancer genomics [16-26].

Clone phylogenies are most often inferred using bulk sequencing data [16, 27-30]. Bulk sequencing of tumor samples is cost effective and can accurately identify single nucleotide variants (SNVs) [31, 32]. The resulting data contains SNV frequencies of cancer cell populations within each tumor sample [27, 33]. Several computational methods have been developed to decompose these SNV profiles into individual clone genotypes, and to predict clone phylogenies [13, 34-39]. These clone genotypes and phylogenies are then employed to infer relative ordering of somatic mutations and to build migration maps of metastatic tumors [40, 41].

Computational methods for clone prediction and phylogeny inference are operationally different from each other. PhyloWGS clusters together SNVs at similar frequencies and then orders them to infer clone genotypes and phylogeny [37]. MACHINA follows a similar process, but also incorporates a model of cancer cell migration between tumor sites (seeding events) [13]. LICHeE generates SNV clusters defined by the pattern of presence and absence of SNVs among tumor samples while considering SNV frequencies [34]. CloneFinder reconstructs ancestral clones in predicting clone genotypes [35]. Treeomics examines the presence and absence of SNVs among tumor samples and resolves evolutionarily incompatible patterns when

bioRxiv preprint doi: https://doi.org/10.1101/697318; this version posted July 19, 2019. The copyright holder for this preprint (which was not certified by peer review) is the author/funder, who has granted bioRxiv a license to display the preprint in perpetuity. It is made available under aCC-BY-NC-ND 4.0 International license.

decomposing SNV profiles into clone genotypes [36]. Ultimately, all of these methods deconvolute individual clones from population bulk sequencing of multiple tumor samples acquired over time and/or different locations in a patient.

Surprisingly, absolute and relative accuracies of clone phylogenies produced by these computational methods have not been assessed using the same collection of datasets, i.e., their performances are yet to be benchmarked. Such benchmarking is critical, because of the biological relevance of the downstream inferences. For example, the accuracies of the order of driver mutations and the interrelationship of clones depend on the performance of current methods in accurately deconvoluting individual clone genotypes and reconstructing evolutionary events. No previous study has evaluated the relative accuracy of clone phylogenetic inferences, as they focused on introducing and assessing the strengths of the new clone prediction methods [13, 34-39]. Besides, the robustness of these computational methods to the complexity of clonal structures and the evolutionary histories of clones from different tumor sites is largely unknown.

Therefore, we evaluated the accuracy of clone phylogenetic inferences by seven clone prediction methods (**Table 1**). We used bulk sequencing datasets simulated under various tumor evolutionary scenarios. Simulated data included small and large numbers of persistent ancestral clones and metastatic tumors that arise from polyclonal seeding events. Our assessments are based on simulation studies because correct phylogenies are known, and computer simulation has emerged as a standard approach for evaluating the performance of statistical methods in cancer genomics [34, 35, 37, 42]. In this study, we identify and highlight the limitations of methods that can most accurately infer clone phylogenies.

Results

We analyzed 150 simulated datasets of tumor bulk sequencing data in which the number of tumor samples ranged from 6 to 11. Tumors and clone sequences were simulated with four distinct

bioRxiv preprint doi: https://doi.org/10.1101/697318; this version posted July 19, 2019. The copyright holder for this preprint (which was not certified by peer review) is the author/funder, who has granted bioRxiv a license to display the preprint in perpetuity. It is made available under aCC-BY-NC-ND 4.0 International license.

models of branching evolution (G7, G12, P10, and MA datasets; **Fig. 1**), and a variety of simulated clone phylogenies (e.g., **Fig. 2**). Details of these simulated datasets are described in the **Methods** section. We inferred clone phylogenies for each simulated dataset by using seven different methods (**Table 1**). We used multiple metrics to assess the accuracy, including those measures that score the correctness of the order of mutations and the branching order within the reconstructed clone phylogenies.

Accuracy of ordering mutations

A clone phylogeny can be viewed as a mutational tree [43] in which all the mutations are mapped along branches (e.g., **Fig. 3**). Such mutational trees can be used to test whether a pair of mutations have occurred concurrently, sequentially, or in parallel (**Fig. 3**). At first, we evaluated the accuracy of the predicted order of mutations by using the MLTED score; a smaller score shows greater similarity between the true and inferred mutational tree (see the **Methods** section for details). We begin with results for G7 and G12 datasets that were modeled after the predicted evolutionary histories of two patients (EV005 and RK26, respectively) (**Fig. 1a-1d**) [35, 44]. Each tumor sample may contain one or a few evolutionarily closely-related clones, assuming a localized genetic heterogeneity [4, 6], i.e., migration of cancer cells to another section of a tumor was assumed to be rare. In total, we obtained 60 simulated datasets (replicates) with 34-89 SNVs per dataset. G7 datasets contained seven tumor samples per dataset, while G12 datasets contained eleven samples. For the G7 datasets, all seven methods showed relatively small MLTED scores. For the G12 datasets, four methods (CloneFinder, MACHINA, Treeomics, and LICHeE) produced much smaller MLTED scores compared to other three (PhyloWGS, MixPhy, and Cloe) (**Fig. 4a**).

The clonal structures of tumors in P10 and MA datasets were more complex than G7 and G12 datasets. The P10 datasets were composed of a few tumor samples, in which ancestral clones were present alongside their descendants (**Fig. 1e** and **1f**). The MA datasets were

bioRxiv preprint doi: https://doi.org/10.1101/697318; this version posted July 19, 2019. The copyright holder for this preprint (which was not certified by peer review) is the author/funder, who has granted bioRxiv a license to display the preprint in perpetuity. It is made available under aCC-BY-NC-ND 4.0 International license.

generated by simulating the evolution of primary and metastatic tumors. The clonal structure of metastatic tumors of some MA datasets was evolutionarily complex, as more than one founding (seeding) clone migrated from another tumor site(s) (e.g., **Fig. 1g** and **1h**). For the P10 and MA datasets, we found that the MLTED scores of Cloe were higher (worse) than other methods (**Fig. 4a**). For the MA datasets, MLTED scores of all the methods were generally higher than the other datasets, and there were large differences among the datasets. Overall, MACHINA and LICHeE showed slightly better performance than the other methods.

Next, we evaluated error rates of ordering sequential, concurrent, and parallel mutations (**Fig. 3**). We generated all possible pairs of SNVs (mutations) and classified them into these three possible categories. In each category, we computed the proportion of real mutation pairs that were not present in the inferred tree, and the proportion of all incorrect mutation pairs. The average of these two proportions was used to assess the error rate of ordering the given type of mutations (see the **Methods** section for details). Sequential and concurrent mutations were inferred with lower accuracy than the parallel mutations (**Table 1**), a difference that was greater for P10 and MA datasets. For example, the error rate of inferring parallel mutations was only 4 – 6% in CloneFinder, MACHINA, Treeomics, and LICHeE analyses for MA datasets, while the error rates for sequential and concurrent mutations were much higher (12 – 21%). Therefore, identification of parallel mutations was generally more reliable than classifying sequential or concurrent mutations.

Accuracy of predicting branching patterns (topology of clone phylogeny)

We next evaluated the accuracy of inferred branching patterns by computing TreeVec and RF distances (see the **Methods** section for details). These distances evaluate the errors of clone groupings in inferred phylogenies. For the G12 datasets (**Fig. 4b**), CloneFinder, MACHINA, Treeomics, and LICHeE showed smaller TreeVec distances than the other methods, i.e., these

bioRxiv preprint doi: https://doi.org/10.1101/697318; this version posted July 19, 2019. The copyright holder for this preprint (which was not certified by peer review) is the author/funder, who has granted bioRxiv a license to display the preprint in perpetuity. It is made available under aCC-BY-NC-ND 4.0 International license.

148 methods produce more accurate branching patterns. Cloe generally showed higher TreeVec
149 distances than other methods. For the G7 datasets, all the methods showed relatively small
150 TreeVec, and indeed, reconstructed clone phylogenies were quite similar to the correct phylogeny
151 for these data (**Additional file 1: Fig. S1**). These patterns are consistent with those based on
152 MLTED scores (**Fig. 4a** and **Table 1**). The results of RF distances were also consistent with
153 MLTED and TreeVec analyses (**Fig. 4c**).

154 ***Impact of persisting ancestral clones***

155 To better understand factors that cause inference errors, we analyzed the impact of the presence
156 of ancestral clones in tumor samples on the accuracy of clone inference. We found that fewer
157 than 50% of the ancestral clones were identified by current methods (**Fig. 5**). Treeomics analysis
158 rarely identified ancestral clones, even in datasets containing as many as six ancestral clones,
159 and MixPhy also performed poorly.

160 All tested methods, except for Cloe, performed well in ordering mutations for a dataset
161 that contained only two ancestral clones (**Fig. 6a**). However, the accuracy of ordering mutations
162 declined when datasets contained tumors with a large number of ancestral clones. In these
163 datasets, CloneFinder, MACHINA, Treeomics, and LICHeE analyses generally had a lower error,
164 indicating their robustness to the presence of persisting ancestral clones within a dataset.

165 For Treeomics, LICHeE, and CloneFinder, the error rate of predicting parallel mutation did
166 not increase significantly with an increasing number of ancestral clones, but the error rates in
167 predicting sequential and concurrent mutations increased significantly (**Fig. 6a**). This is because
168 the inability to detect ancestral clones would misclassify sequential mutations as concurrent
169 mutations (e.g., **Additional file 1: Fig. S2**).

bioRxiv preprint doi: https://doi.org/10.1101/697318; this version posted July 19, 2019. The copyright holder for this preprint (which was not certified by peer review) is the author/funder, who has granted bioRxiv a license to display the preprint in perpetuity. It is made available under aCC-BY-NC-ND 4.0 International license.

Consistent with the ability to predict correct mutation orders, all tested methods (except for Cloe) showed relatively small TreeVec and RF distances when a dataset contained only two ancestral clones (**Fig. 6b**), while CloneFinder, MACHINA, Treeomics, and LICHeE generally produced smaller TreeVec and RF distances for datasets with larger numbers of ancestral clones. Overall, no method produced highly accurate clone phylogenies for datasets containing a large number of ancestral clones.

Impact of polyclonal seeding events during metastatic tumor evolution

The analysis of MA datasets was used to assess the impact of polyclonal seeding of metastatic tumors on clone phylogeny and mutation orders. These datasets contained primary tumors and four or six metastatic tumors. Up to four metastatic tumors per dataset evolved with polyclonal seeding events, i.e., these metastatic tumors were founded by more than one seeding clone. When a metastatic tumor received more than one seeding clone (polyclonal seeding events), these tumors contained clones from different evolutionary lineages due to distinct founder (seeding) clones (e.g., **Fig. 1g** and **1h**). No tested method was able to accurately identify a majority of clones within multiple-seeded metastatic tumors (**Fig. 7a**). MACHINA is the only method that incorporates the metastatic progression model of clone seeding events during its estimation process, and it did outperform other tested methods when datasets contained the largest number of multiple-seeding events (**Fig. 7a**). Overall, the poor performance of all the methods in inferring clones resulted in higher error rates of ordering mutations and reconstructing branching patterns (**Fig. 7b-7g**).

Even when a MA dataset contained only one polyclonal seeding event in a metastatic tumor, we observed errors in phylogenetic predictions, mainly caused by unsuccessful inference of clones' presence within that metastatic tumor. For example, **Figure 8** shows inferred clone phylogenies for an example dataset (**Fig. 1g** and **1h**) in which a metastatic tumor (M5)

bioRxiv preprint doi: https://doi.org/10.1101/697318; this version posted July 19, 2019. The copyright holder for this preprint (which was not certified by peer review) is the author/funder, who has granted bioRxiv a license to display the preprint in perpetuity. It is made available under aCC-BY-NC-ND 4.0 International license.

194 experienced polyclonal seeding events such that two seeding clones came from two distinct clone
195 lineages (clone lineage C/D, which contained clone C and D, and lineage M with clone M). All the
196 methods, including MACHINA, identified only one out of these two clone lineages (lineages C/D
197 or M), with MACHINA producing two solutions (**Fig. 8b** and **8c**). The first solution contained only
198 clone C, whereas the second solution contained only clone M. In these MACHINA phylogenies,
199 these two clones were connected with erroneously long branches (**Fig. 1g**). Thus, those correct
200 clones found within the M5 metastatic tumor were convoluted into one clone genotype in the
201 inferred clone phylogenies. This same type of error was observed in predicted clone phylogenies
202 generated via other methods (**Fig. 8**), except for Cloe (which produced phylogenies that
203 dramatically differed from the true phylogeny). Apart from these errors, the predicted clone
204 phylogenies were largely similar to the true clone phylogeny, and the branching patterns were
205 mostly correct (**Fig. 1** and **Fig. 8**). For this example MA dataset, MACHINA, CloneFinder, and
206 LICHeE produced more accurate clone phylogenies than other methods. For example,
207 Treeomics, PhyloWGS, and MixPhy produced much smaller phylogenies, as these methods did
208 not infer many ancestral or highly-similar clones.

209 This pattern of errors in inferred clone phylogenies became more acute when a dataset
210 included many metastatic tumors that evolved with polyclonal seeding events. For example, when
211 a dataset was composed of four metastatic tumors with polyclonal seeding events, inferred clone
212 phylogenies contained fewer clones than the true phylogeny (**Additional file 1: Fig. S3**). The
213 tested methods tended to predict only one clonal lineage for each of the four metastatic tumors
214 of this dataset. Note that Cloe produced a phylogeny with little similarity to the true phylogeny.
215 MACHINA produced 870 solutions for this example dataset, with the best solution (smallest
216 number of SNV assignment errors per clone) similar to the true phylogeny, and the worst solution
217 that missed many clonal lineages. Overall, current clone prediction methods cannot reliably
218 decompose many clones within metastatic tumors with polyclonal seeding events.

bioRxiv preprint doi: https://doi.org/10.1101/697318; this version posted July 19, 2019. The copyright holder for this preprint (which was not certified by peer review) is the author/funder, who has granted bioRxiv a license to display the preprint in perpetuity. It is made available under aCC-BY-NC-ND 4.0 International license.

Empirical data analysis

The application of these clone prediction methods to an empirical dataset (A7 dataset from a previous study [30]) showed results consistent with our analyses of simulated data. The original study reported that metastatic rib and lung tumors harbored clones from different clonal lineages (**Fig. 9a**). The lung tumor contained three different clone lineages, indicating a complicated history of metastatic tumor evolution. Different methods predicted clone phylogenies that showed limited similarity to the clone phylogeny reported in the original study (**Fig. 9b-9i**). MACHINA produced four similar solutions (**Fig. 9b-9e**). However, only the predicted evolutionary relationship of clones from liver and kidney tumors agreed with those reported in the original study [30]. The predicted clone sharing between lung and brain tumors reported by CloneFinder agreed with the original study, but the clone phylogeny differed dramatically (**Fig. 9f**). Treeomics correctly predicted the evolutionary relationship of clones from the liver, kidney, and rib tumors, but did not predict most of the ancestral clones (**Fig. 9g**), a failing that we also observed in our simulation results. PhyloWGS produced two distinct but highly similar clone phylogenies (**Fig. 9h** and **9i**) that indicated the presence of three clonal lineages, instead of the two lineages reported in the original study. LICHeE analyses did not produce a solution. MixPhy produced >400 clones for this dataset, and Cloe results suggested the unlikely scenario that all predicted clones were present in most of the samples. Therefore, we anticipate that the application of different computational methods in actual empirical data analysis will result in widely varying inferences, making it challenging to reach reliable biological conclusions, when the tumor evolution is highly complex.

Discussion

Predictions of accurate clone phylogenies are essential to infer the order of driver mutation occurrences and the evolutionary relationship of clones. We tested the accuracy of published

bioRxiv preprint doi: https://doi.org/10.1101/697318; this version posted July 19, 2019. The copyright holder for this preprint (which was not certified by peer review) is the author/funder, who has granted bioRxiv a license to display the preprint in perpetuity. It is made available under aCC-BY-NC-ND 4.0 International license.

methods in reconstructing clone phylogenies as a first step in identifying the patterns of errors in clone phylogeny inference, which revealed some useful guidelines for applying computational methods in practical data analysis. To begin with, we suggest the use of CloneFinder, MACHINA, Treeomics, and LICHeE, because they often showed lower error rates of ordering mutations and inferring phylogenies. All of these methods benefit from the use of intrinsic evolutionary relationship of tumor clones. The evolutionary information provides resolution beyond inferences primarily based on the dissimilarities of observed SNV frequencies because low read depth cause SNV frequencies to have significant variance and clone predictions based on only the similarities of observed SNV frequencies become error-prone.

Careful consideration of the input data is strongly recommended before choosing a method for analyses. First, these clone prediction methods require copy-number-neutral SNVs, because observed SNV frequencies are affected by copy number alterations (CNAs). SNV frequencies should be adjusted to eliminate the impact of CNAs. Notably, Cloe [39] is designed for the analysis of datasets with CNAs, but it did not perform well for datasets without CNAs.

Also, most methods are known not to be robust to the presence of incorrect SNV assignments, so one should proceed with extreme caution when analyzing datasets with high rates of sequence error. For example, LICHeE may fail to produce any inferences on such datasets or the accuracy may become much lower than other methods (e.g., Treeomics) [35]. LICHeE failed to produce any results for our example empirical dataset [30]. In general, clone predictions are expected to become more challenging when the dataset contains CNAs and sequencing errors. Also, the accuracy of clone phylogeny inference can be adversely impacted by biological factors (e.g., the impact of strong natural selection).

Another important consideration in experimental design is the benefit of sequencing a larger number of tumor samples. The most successful methods in our evaluations use the intrinsic

bioRxiv preprint doi: https://doi.org/10.1101/697318; this version posted July 19, 2019. The copyright holder for this preprint (which was not certified by peer review) is the author/funder, who has granted bioRxiv a license to display the preprint in perpetuity. It is made available under aCC-BY-NC-ND 4.0 International license.

267 evolutionary relationships among tumor samples so a larger sample number can provide more
268 information to improve clone predictions. All of the methods tested here performed well on
269 simulated datasets with the largest number of tumor samples (G12 datasets). Although the actual
270 number of tumor samples preferred depends on the situation, it is clear that one should avoid
271 datasets generated from only a few samples. Importantly, datasets with a very small number of
272 samples will underestimate the genetic heterogeneity of a tumor site, and therefore, the use of a
273 large number of samples per patient is a standard recommendation [6, 45].

274 We do not expect any of the currently available methods to be effective in situations where
275 each tumor sample contains clones from many lineages (if tumors frequently exchange clones).
276 We have previously documented that CloneFinder will not perform well on such datasets [35].
277 Also, our simulation analyses have shown that none of the tested methods perform well when a
278 mixture of clones from different evolutionary lineages exist within metastatic tumors (multiple
279 seeding).

280 Lastly, we suggest using multiple methods to infer clone phylogenies and examining the
281 consistency among the results. We found that the best performing methods produced similar
282 results when inferred clone phylogenies were accurate. When using Treeomics, it is crucial to be
283 aware that the inferred clone phylogenies will not include most of the ancestral clones. Also,
284 potential errors on clonal lineage deconvolution can be detected when MACHINA produces at
285 least two disparate clone phylogenies (e.g., **Fig. 8**) or when MACHINA produces hundreds of
286 solutions. In general, the inconsistency of inferred clone phylogenies suggests the influence of
287 complicated clonal structures within tumors, i.e., a mixture of different lineage clones. Currently,
288 no method can produce accurate clone phylogenies from such data. Thus, consistency among
289 inferred phylogenies may be useful to validate inferences.

bioRxiv preprint doi: https://doi.org/10.1101/697318; this version posted July 19, 2019. The copyright holder for this preprint (which was not certified by peer review) is the author/funder, who has granted bioRxiv a license to display the preprint in perpetuity. It is made available under aCC-BY-NC-ND 4.0 International license.

In summary, we can accurately infer clone phylogenies only when tumor evolution generally tracks clonal evolution, a relationship that is disrupted when tumors exchange clones reduce the quality of the inferred clone phylogenies. Also, ancestral clones that persist alongside the descendant clones within a tumor sample are difficult to identify, leading to inaccuracy in the reconstruction of evolutionary events.

Conclusions

Analyses of correct clone phylogenies are critical to a better understanding of tumor evolution and the influence of genetic heterogeneity. We recommend clone prediction methods that use the intrinsic evolutionary relationship of tumor samples (e.g., CloneFinder, MACHINA, TreeOmics, and LICHeE). The inferences of multiple methods should also be compared to validate predictions. There is a strong need for more advanced methods that can perform well for datasets with intermixing of tumor samples.

Methods

Generation of bulk sequencing data

We analyzed 150 simulated datasets that were available from published studies in which the accuracy of inferred clone sequences was assessed [13, 35]. Each dataset contained information on mutant and wild-type read counts (with read counting errors).

G7 and G12 datasets. These datasets contained seven and twelve clones, respectively, modeled after the predicted evolutionary histories of two patients (EV005 and RK26 [44], respectively) (**Fig. 1a-1d**) [35]. Each tumor sample may contain one or a few evolutionarily closely-related clones, assuming a localized genetic heterogeneity due to branching evolution [4, 6]. Thus, the migration

bioRxiv preprint doi: https://doi.org/10.1101/697318; this version posted July 19, 2019. The copyright holder for this preprint (which was not certified by peer review) is the author/funder, who has granted bioRxiv a license to display the preprint in perpetuity. It is made available under aCC-BY-NC-ND 4.0 International license.

of cancer cells to another section of a tumor was assumed to be rare in these datasets. In total, we obtained 60 simulated datasets (replicates) with 34-89 SNVs per dataset.

P10 datasets. In these datasets, various numbers of clones persisted within a sector (sample) of a tumor after the origin of descendant clones. Ten random clone phylogenies were simulated, and every tumor sample was populated with one tip clone and its ancestral clones ("localized sampling process" [34]) (**Fig. 1e** and **1f**). Each of P10 datasets contained 2 – 6 ancestral clones (30 datasets). A selection of simulated clone phylogenies is shown in Figure 3 of Miura et al. [35].

MA datasets. These datasets were generated by modeling the evolution of primary and metastatic tumors (four or seven metastatic tumors per dataset) [13]. Metastatic tumors were founded by cancer cells (seeding clones) that migrated from another tumor site (primary or another metastatic tumor). Under a simple metastatic tumor evolution scenario, each metastatic tumor received a single founder (seeding) clone from another tumor site, and a metastatic tumor contained only clones that evolved from a single seeding clone. Clonal structures of metastatic tumors became more complicated when a metastatic tumor was seeded by more than one clone (polyclonal seeding events). In MA datasets, a metastatic tumor received a maximum of two seeding clones, and any dataset may contain more than one metastatic tumor with polyclonal seeding events. Thus, the observed genotypes of these metastatic tumors represented two convoluted clone lineages, and clone prediction methods were required to correctly identify such tumors and decompose them into two distinct clone lineages (e.g., **Fig. 1g** and **1h**). Each MA dataset contained up to four metastatic tumors with polyclonal seeding events. Each clone phylogeny was unique (60 MA datasets). All the clone phylogenies are shown in **figure 2**.

Selection of clone prediction methods and parameter settings

We selected clone prediction methods that have performed well in predicting clone genotypes from observed SNV frequencies or read counts of bulk sequencing data [35]. That is, we excluded

bioRxiv preprint doi: https://doi.org/10.1101/697318; this version posted July 19, 2019. The copyright holder for this preprint (which was not certified by peer review) is the author/funder, who has granted bioRxiv a license to display the preprint in perpetuity. It is made available under aCC-BY-NC-ND 4.0 International license.

methods that produce highly incorrect clone genotypes because such clone genotypes do not produce correct clone phylogenies. By this criterion, we excluded CITUP [46], BayClone2 [47], Clomial [48], Canopy [49], cloneHD [50], and AncesTree [51] (see **Additional file 1: Table S1** for the average number of SNV assignment errors per clone). We did not include methods that require prior information of the composition of SNV clusters (e.g., TrAp [52]) or those that require the use of another software to produce clone genotypes by ordering predicted clusters (e.g., PyClone [53] and SciClone [54]). Lastly, we did not include methods that were designed for the analyses of single-cell sequencing data (e.g., SCITE [55] and BEAM [56]), because clone deconvolution is not necessary for this type of data, while these methods focus on imputing missing data and minimizing SNV assignment errors in the inference of cell phylogenies [31, 32]. These considerations resulted in the selection of seven clone prediction methods (**Table 1**) [13, 34-39]. Each method was used with its default or recommended parameter settings. In MA datasets, we found many similar clone genotypes, so we used parameter settings that can differentiate similar clone genotypes. This modification was applied only for LICHeE and CloneFinder, as only these two methods include options for this purpose.

MACHINA [13]. We used the PMH-TI mode in the MACHINA software, which infers clone genotypes from read count data. The MACHINA software requires *a priori* identification of tumor sites as primary or metastatic for each sample. Since G7, G12, and P10 datasets were simulated without the consideration of primary and metastatic tumor evolution, we assumed that the primary tumor contained the root clone (e.g., clone A for G7 and G12 datasets) (**Fig. 1a and 1c**). When a root clone was not present in a dataset, we selected the clone that was most closely located to the root of a simulated phylogeny. For MA datasets, we provided the correct tumor site (primary or metastatic site, in which distinct metastatic tumor sites were accordingly distinguished) for each clone sequence that was found. Note that MACHINA often produced a large number of solutions (>10 solutions per dataset) for G7, G12 and MA datasets. In those cases, we first identified the

bioRxiv preprint doi: https://doi.org/10.1101/697318; this version posted July 19, 2019. The copyright holder for this preprint (which was not certified by peer review) is the author/funder, who has granted bioRxiv a license to display the preprint in perpetuity. It is made available under aCC-BY-NC-ND 4.0 International license.

best and worst solutions for each dataset, which were determined based on the average number of SNV assignment errors per clone. We reported the average error rate (see below) of the best and worst solutions.

LICHeE [34]. Following the default settings, we set the variant allele frequency (VAF) error margin the value 0.1. SNVs were considered robustly present in a sample at VAF > 0.005 (robust SNVs), and the others were considered absent in a sample. SNVs with VAF > 0.6 were excluded. LICHeE groups SNVs based on the pattern of presence/absence of mutations across the samples and each SNV group was required to contain at least two robust SNVs. LICHeE also clusters SNVs by VAF similarities. We required that an SNV cluster contained at least two SNVs unless an SNV was sample specific. All the SNV groups/clusters were initially kept in the network. Two groups/clusters could collapse when mean VAF difference was < 0.2.

LICHeE did not produce clonal compositions of samples (i.e., clone frequencies). Thus, we estimated clone frequencies using the relationship $½f \times M = V$, where f is a two-dimensional matrix of estimated clone frequencies of the samples, M is a matrix of predicted clone genotypes, and V is the observed SNV frequency [33]. The equation above applies to cases where the variants are free of copy number alterations (CNAs) [33], which is the case for our datasets. We estimated f through the regression of V to a function of M and f [57]. Clone frequencies were estimated excluding SNVs with small total read count (<50) and mutant read count (<2), because those observed SNV frequencies were not reliable. When ancestral clones were predicted to co-exist with their descendant clones within a sample, we tested if these ancestral clones were spurious. Between a pair of ancestral and descendant clones, we compared observed SNV frequencies that are unique to the descendant clone and those shared with the ancestral clone. We used the expectation of higher observed SNV frequencies on shared (mutations that were found in both clones) than on unique mutations (mutations that were found in only a descendant clone; *t*-test)

bioRxiv preprint doi: https://doi.org/10.1101/697318; this version posted July 19, 2019. The copyright holder for this preprint (which was not certified by peer review) is the author/funder, who has granted bioRxiv a license to display the preprint in perpetuity. It is made available under aCC-BY-NC-ND 4.0 International license.

to discover the spurious presence of ancestral clones. When the differences between SNV frequencies were not significant ($P > 0.05$), the ancestral clones were removed. Also, we discarded clones present at low frequencies (<2%).

In the analyses of MA datasets, only SNVs with zero SNV frequency were considered to be robustly absent from a sample, and SNVs with > 0.0001 frequency were considered to be robustly present in a sample (robust SNVs). All SNVs were examined regardless of their observed frequency. The minimum number of SNVs per cluster/group was set to one. Two SNV clusters were collapsed when mean SNV frequency differences were less than 1%. We did not discard any ancestral clones.

CloneFinder [35]. We estimated clone genotypes using SNVs with at least 50 reference read counts and two mutant read counts, and we discarded clones when estimated clone frequencies were < 2%. To analyze MA datasets, we did not combine similar clone genotypes or discard clones. We used all reads.

Treeomics [36]. We used the option of enabling subclone detection.

PhyloWGS [37]. The fraction of expected reference allele sampling from the reference population and the variant population were 0.999 and 0.4999, respectively. We set copy number equal to one (heterozygous mutant allele). As PhyloWGS did not produce clone frequencies, we computed clone frequencies using the approach described for LICHeE (see above).

Mixed Perfect Phylogeny (MixPhy) [38]. We performed analyses in MixPhy (v0.1) with the option of a heuristic algorithm. As the input file requires a binary matrix of tumor sample genotypes (presence/absence of mutation), we provided correct sample genotypes, assuming that there were no false positive or false negative detections of mutations.

bioRxiv preprint doi: https://doi.org/10.1101/697318; this version posted July 19, 2019. The copyright holder for this preprint (which was not certified by peer review) is the author/funder, who has granted bioRxiv a license to display the preprint in perpetuity. It is made available under aCC-BY-NC-ND 4.0 International license.

Cloe [39]. We applied Cloe with 10,000 iterations and 4 MCMC parallel chains at temperatures of 1, 0.9, 0.82, and 0.75. For the posterior evaluation of MCMC sampled trees, the burn-in of MCMC chains was 0.5, and chain thinning was 4. The maximum number of clones for a dataset was set to the true clone count.

Evaluation of predicted clone phylogenies

We compared each predicted clone phylogeny with the respective true clone phylogeny by using the following four metrics.

Multi-labeled tree edit distance (MLTED) [58]. A clone phylogeny is often viewed as a mutational tree [43] in which all the mutations are mapped along branches. Mutational trees are useful when the number of tips in the inferred clone phylogeny differs from the true phylogeny and when the sequences of the inferred clones do not match all the true clones. We used the Multi-labeled Tree Edit Distance (MLTED score) for comparing the inferred and the true tree, as it has been designed to evaluate clone trees [58], available at https://github.com/khaled-rahman/MLTED. This algorithm requires that the inferred tree contains the same set of mutations as in the true tree. Because of errors in clone sequence predictions, some mutations were not assigned to any branch in the inferred tree. These mutations were placed at the root of the inferred mutational tree.

The error rate of ordering mutations. We generated all possible pairs of SNVs (mutations) and classified them into three possible types, i.e., concurrent, sequential, and parallel (see **Fig. 3** for examples). Concurrent mutations are those that occurred on the same branch (irrespective of their order), whereas sequential and parallel mutations are those that occurred on different branches of the clone phylogeny. More specifically, two mutations are sequential if one occurred on the ancestral branch and the other on its descendant branch, but multiple intervening branches may separate them. Two mutations are parallel if they are found on sibling lineages that have

bioRxiv preprint doi: https://doi.org/10.1101/697318; this version posted July 19, 2019. The copyright holder for this preprint (which was not certified by peer review) is the author/funder, who has granted bioRxiv a license to display the preprint in perpetuity. It is made available under aCC-BY-NC-ND 4.0 International license.

descended from their most recent common ancestor. Any true mutation pair not found in the inferred tree was classified as “unassigned.”

We estimate the error rate of ordering concurrent, sequential, and parallel mutations, separately. In each category, we first scored the number of true mutation pairs that were not present in the inferred tree and divided it by the total number of true mutation pairs. Then, we scored the number of mutation pairs that were incorrect and divided it by the total number of inferred mutation pairs. Then, the average of these two proportions was used as the error rate of ordering the given type of mutations. Similar measures have been used to evaluate clone prediction methods in previous studies [34].

Advanced Tree vector (TreeVec) [59]. We also evaluated the accuracy of branching patterns (topology) in inferred clone phylogenies (clonal lineage trees [43]). For this purpose, we first mapped inferred clone genotypes to the true clone genotypes, because inferred clone genotypes never perfectly match the true clone genotypes. We mapped each inferred clone genotype to its most similar true clone genotype in a two-step process. First, each true clone genotype was compared to all the inferred clone genotypes, and the two clones with the smallest difference were paired. When the number of inferred clones was greater than the number of true clones, the remaining inferred clones were paired with the most similar true clone genotype. For uniformity, we reconstructed inferred clone phylogenies by using predicted clone genotypes produced by each method. Because mutations arose only once in the computer simulated data, the maximum parsimony analysis was suitable [60] and was performed using MEGA-CC [61]. All the clone phylogenies were rooted using germline sequences (normal cells) as outgroups. In inferred clone phylogenies, we labeled tips with clone annotations. When an inferred clone genotype had two different annotations, we duplicated the genotype in an inferred clone phylogeny, i.e., the

bioRxiv preprint doi: https://doi.org/10.1101/697318; this version posted July 19, 2019. The copyright holder for this preprint (which was not certified by peer review) is the author/funder, who has granted bioRxiv a license to display the preprint in perpetuity. It is made available under aCC-BY-NC-ND 4.0 International license.

corresponding tip was duplicated. Also, two inferred clone genotypes might have the same annotation. In this case, two tips in an inferred clone phylogeny were labeled identically.

Among various tree distance computation methods for phylogenies [62], we selected the advanced TreeVec distance developed by Kendall et al. [59], because TreeVec allowed more than one tip with identical labels. Briefly, TreeVec distance computation first collapsed any monophyletic clade(s), i.e., a clade with tips that had an identical label. Then, the traditional TreeVec distance [63] was computed, which counted the number of branches (edges) between the root and the node of the most recent common ancestor (MRCA) of a pair of clones. For all pairs of clones, the Euclidean metric between inferred and true counts was computed. We used the treespace software [64] to compute this advanced TreeVec distance.

Robinson and Foulds (RF) distance [65]. We also computed RF tree distance, because it is widely applied in the evaluation of species phylogenies. We used PhyloNET software [66] to count the number of partitions that were common and different between the true and the inferred phylogeny. The RF distance is the number of differing partitions divided by the total number of partitions in the two phylogenies. Note that RF distance computation requires that both the inferred and the true clone phylogenies contain the same number of tips (clones). However, inferred clone phylogenies may contain more tips than the respective true phylogenies, when more than one tip is assigned an identical clone annotation (i.e., more than one inferred clone genotype was similar to a true genotype). When there were too many tips in the inferred tree, we retained only those tips that showed the highest similarity to the true clone genotypes, such that each true clone genotype was matched with exactly one inferred genotype.

Empirical data analyses

We obtained an empirical dataset (patient A7 dataset [30]; https://github.com/raphael-group/machina), which contained genotypes for 478 copy-neutral SNVs. This dataset contains

bioRxiv preprint doi: https://doi.org/10.1101/697318; this version posted July 19, 2019. The copyright holder for this preprint (which was not certified by peer review) is the author/funder, who has granted bioRxiv a license to display the preprint in perpetuity. It is made available under aCC-BY-NC-ND 4.0 International license.

478 SNV frequencies of one primary tumor sample (breast) and four metastatic tumors (lung, liver,
479 rib, and brain), for which clone phylogenies and clonal composition of each sample have been
480 previously reported [30]. For real data, true clone genotypes are not available, so we annotated
481 each clone on the inferred phylogeny based on the sample(s) that contained it (**Fig. 9a**) in order
482 to compare the reported phylogeny [30] with those inferred by the clone prediction methods listed
483 in **Table 1**.

484

485

bioRxiv preprint doi: https://doi.org/10.1101/697318; this version posted July 19, 2019. The copyright holder for this preprint (which was not certified by peer review) is the author/funder, who has granted bioRxiv a license to display the preprint in perpetuity. It is made available under aCC-BY-NC-ND 4.0 International license.

Table

Table 1. Error rates of methods in inferring sequential, parallel, and concurrent mutations.

	Method						
Mutation type	CloneFinder	MACHINA	TreeOmics	LICHeE	MixPhy	PhyloWGS	Cloe
G7 dataset							
Sequential	4%	7%	5%	17%	9%	15%	10%
Parallel	3%	6%	4%	19%	9%	25%	12%
Concurrent	2%	4%	10%	20%	10%	13%	14%
G12 dataset							
Sequential	1%	7%	6%	5%	38%	37%	44%
Parallel	0%	4%	4%	3%	15%	34%	49%
Concurrent	1%	5%	12%	0%	0%	27%	62%
P10 dataset							
Sequential	10%	15%	11%	7%	17%	21%	32%
Parallel	3%	5%	1%	1%	6%	9%	21%
Concurrent	11%	17%	13%	10%	11%	13%	47%
MA dataset							
Sequential	19%	12%	18%	21%	32%	28%	64%
Parallel	5%	4%	6%	5%	7%	11%	21%
Concurrent	20%	14%	20%	17%	20%	21%	86%
Average	6%	8%	9%	11%	15%	21%	38%

Note.- See the **Methods** section for details about the calculation of error rates.

bioRxiv preprint doi: https://doi.org/10.1101/697318; this version posted July 19, 2019. The copyright holder for this preprint (which was not certified by peer review) is the author/funder, who has granted bioRxiv a license to display the preprint in perpetuity. It is made available under aCC-BY-NC-ND 4.0 International license.

Figures

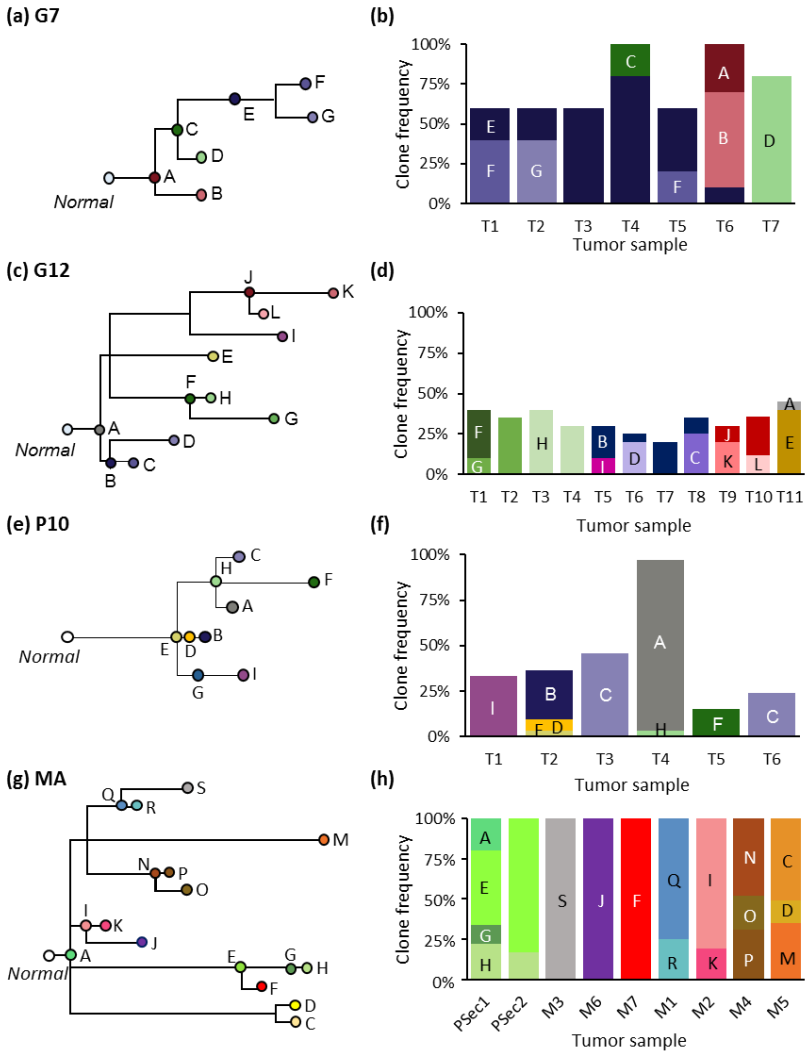

Figure 1. Simulated clone phylogenies and tumor composition. (**a and b**) A phylogeny, and clone frequencies of seven clones and seven tumor samples (T1-T7) derived from EV005 tree (G7 datasets) [44]. (**c** and **d**) A phylogeny and clone frequencies of twelve clones and eleven tumor samples (T1-T11) derived from RK26 tree (G12 datasets) [44]. (**e** and **f**) One of thirty phylogenies and its tumor composition from P10 datasets [35]. (**g** and **h**) One example of MA datasets (out of the 60) with primary tumor (PSec1 and PSec2) and metastatic tumors (M1-M5) [13]. Note that tumor purities are 100% for all the samples.

bioRxiv preprint doi: https://doi.org/10.1101/697318; this version posted July 19, 2019. The copyright holder for this preprint (which was not certified by peer review) is the author/funder, who has granted bioRxiv a license to display the preprint in perpetuity. It is made available under aCC-BY-NC-ND 4.0 International license.

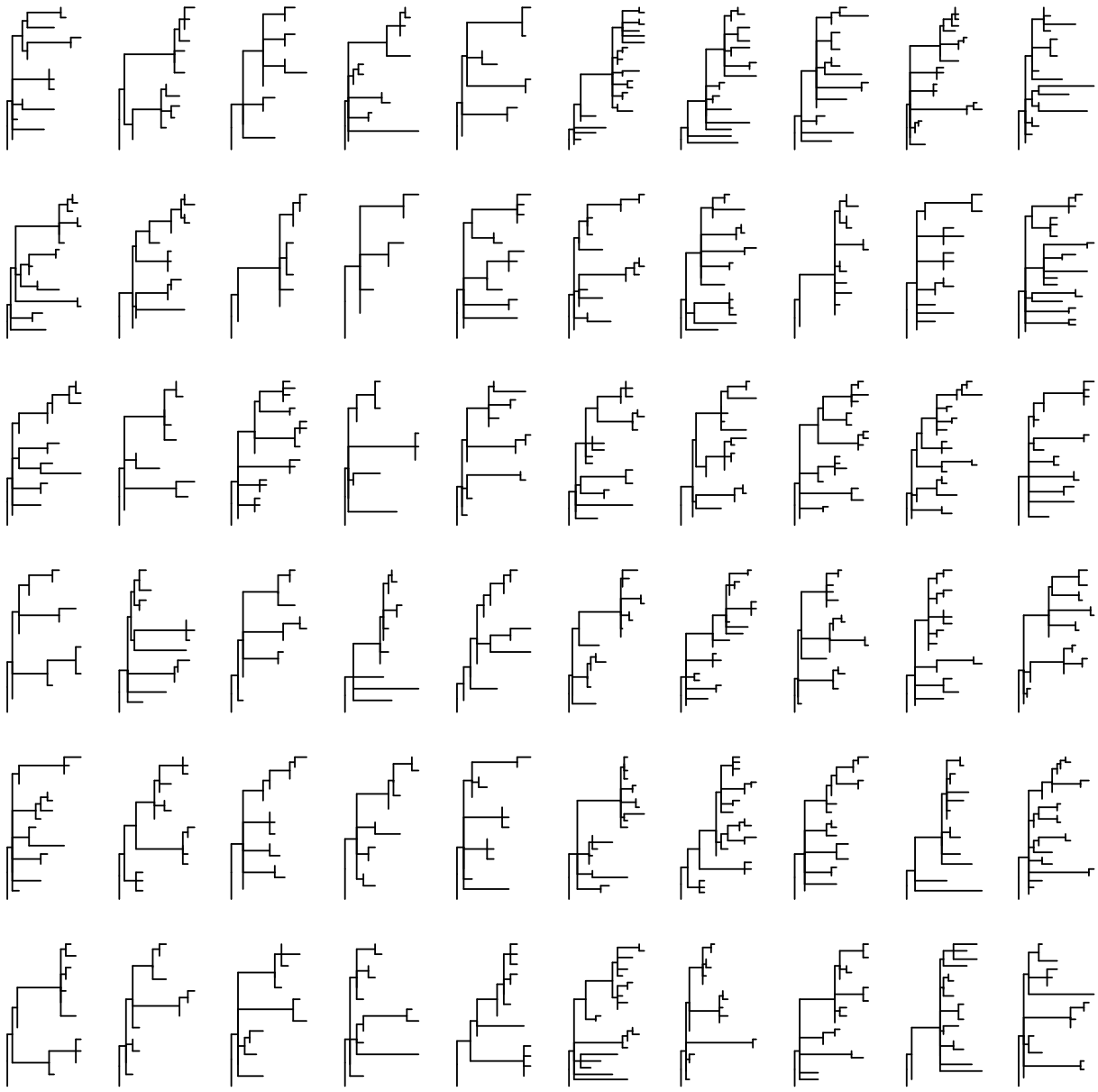

Figure 2: Clone phylogenies used for simulating MA datasets. All clone phylogenies were different.

bioRxiv preprint doi: https://doi.org/10.1101/697318; this version posted July 19, 2019. The copyright holder for this preprint (which was not certified by peer review) is the author/funder, who has granted bioRxiv a license to display the preprint in perpetuity. It is made available under aCC-BY-NC-ND 4.0 International license.

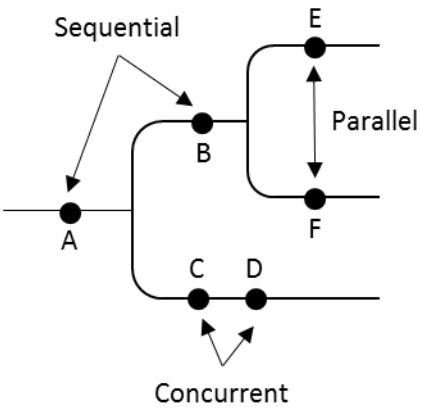

504

505 **Figure 3**: A mutational tree with concurrent (e.g., C and D), sequential (e.g., A and B), and parallel

506 (e.g., E and F) mutations. Dots depict mutations. Order of mutations on a branch (e.g., C and D)

507 cannot be determined based on the clone phylogeny alone.

508

bioRxiv preprint doi: https://doi.org/10.1101/697318; this version posted July 19, 2019. The copyright holder for this preprint (which was not certified by peer review) is the author/funder, who has granted bioRxiv a license to display the preprint in perpetuity. It is made available under aCC-BY-NC-ND 4.0 International license.

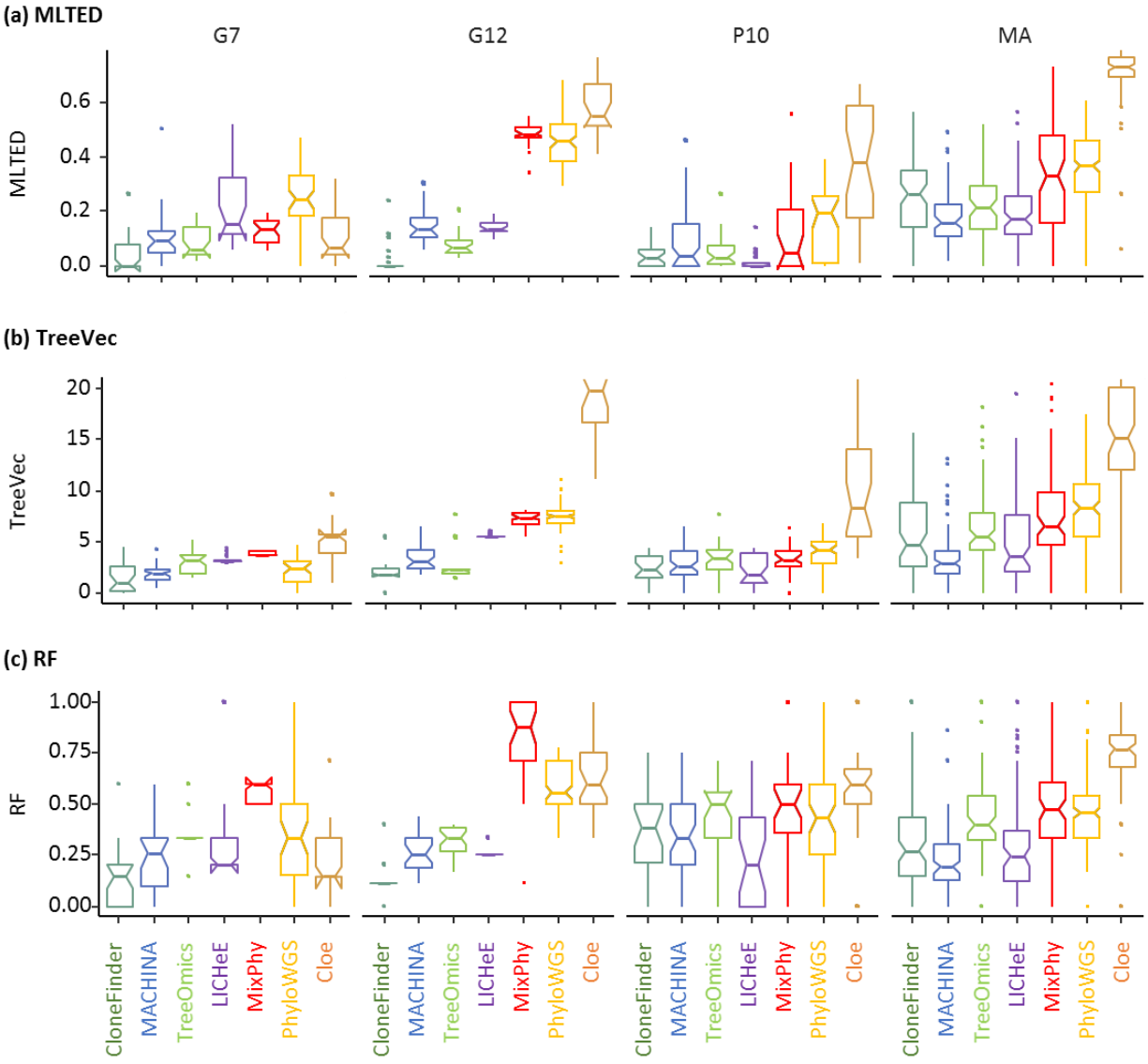

509

510 **Figure. 4**. Performance of seven methods measured by (**a**) MLTED, (**b**) TreeVec, and (**c**) RF

511 distances. MLTEDs show the accuracy of inferred mutation orders, whereas TreeVec and RF the

512 accuracy of inferred clone phylogenies (small values indicate higher accuracy).

513

bioRxiv preprint doi: https://doi.org/10.1101/697318; this version posted July 19, 2019. The copyright holder for this preprint (which was not certified by peer review) is the author/funder, who has granted bioRxiv a license to display the preprint in perpetuity. It is made available under aCC-BY-NC-ND 4.0 International license.

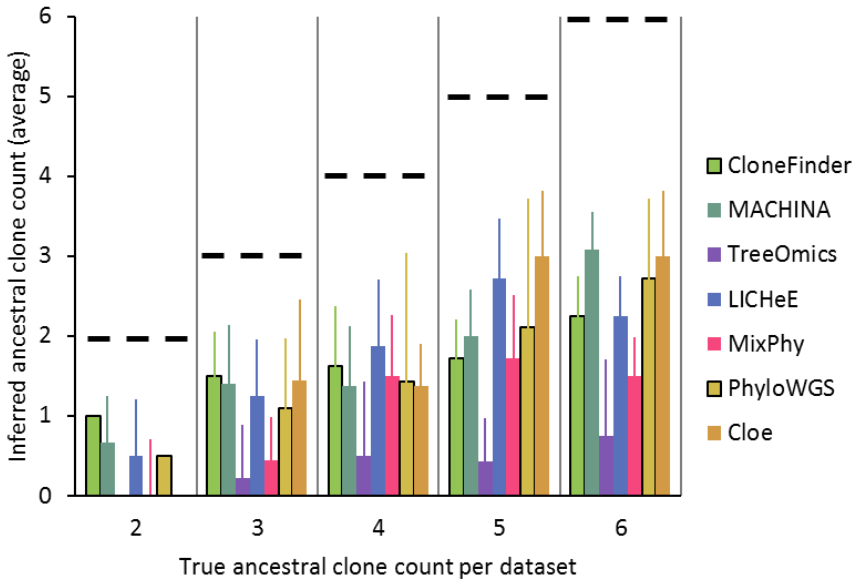

514

515 **Figure 5**: The average number of ancestral clones that were identified per dataset for the P10
516 datasets. We grouped P10 datasets based on the true number of ancestral clones in a dataset.
517 For each dataset, we counted the number of ancestral clones identified by a clone prediction
518 method. We then computed the average across the dataset. Dashed lines are the correct count.
519 Error bars represent standard deviation values.

520

bioRxiv preprint doi: https://doi.org/10.1101/697318; this version posted July 19, 2019. The copyright holder for this preprint (which was not certified by peer review) is the author/funder, who has granted bioRxiv a license to display the preprint in perpetuity. It is made available under aCC-BY-NC-ND 4.0 International license.

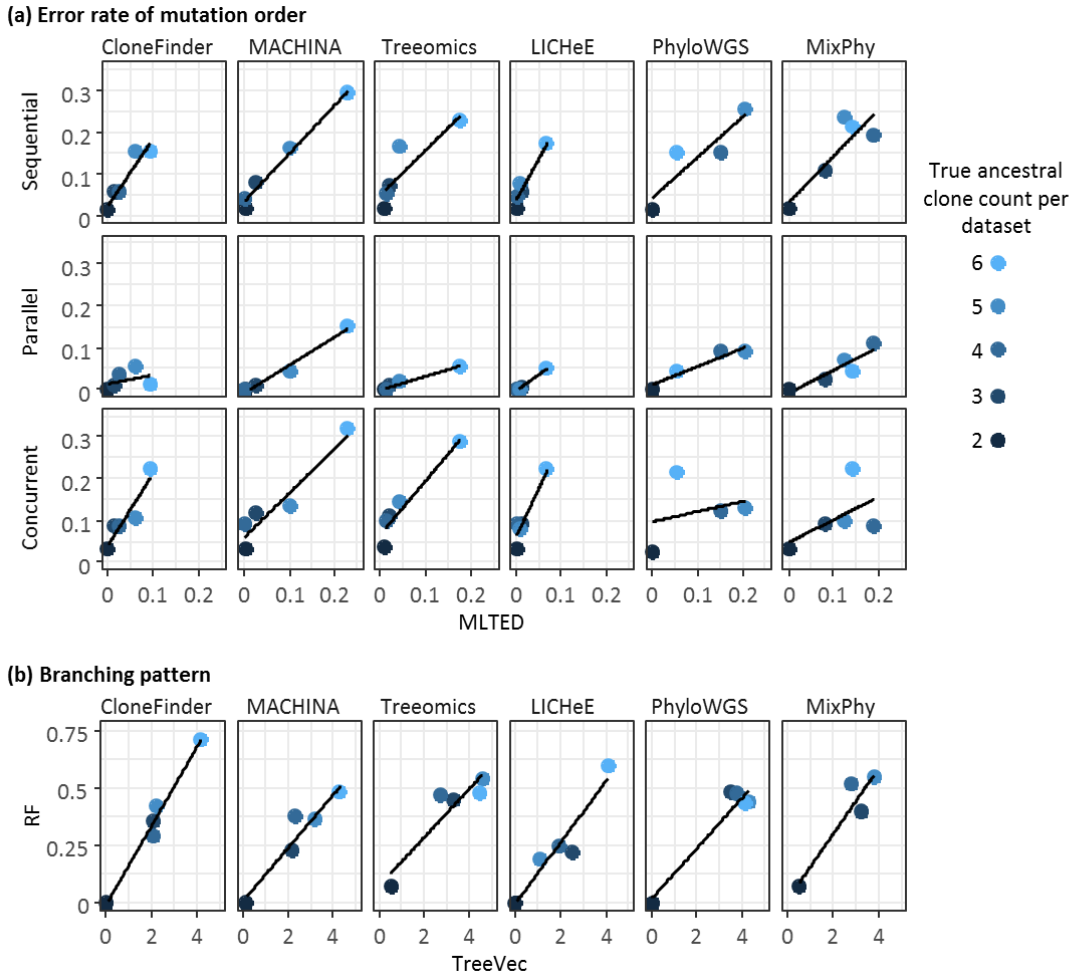

Figure 6: Accuracy of ordering mutations and inferring branching patterns, when a dataset contained various number of of ancestral clones. P10 datasets were used and were grouped based on the true ancestral clone count in a dataset. Each point shows the average of tree distance across the datasets. (**a**) The average error rate of ordering mutations and MLTED. (**b**) RF distances and TreeVec. Cloe method was excluded because both MLTED scores and average error rates were very high (**Fig. 4** and **Table 1**).

bioRxiv preprint doi: https://doi.org/10.1101/697318; this version posted July 19, 2019. The copyright holder for this preprint (which was not certified by peer review) is the author/funder, who has granted bioRxiv a license to display the preprint in perpetuity. It is made available under aCC-BY-NC-ND 4.0 International license.

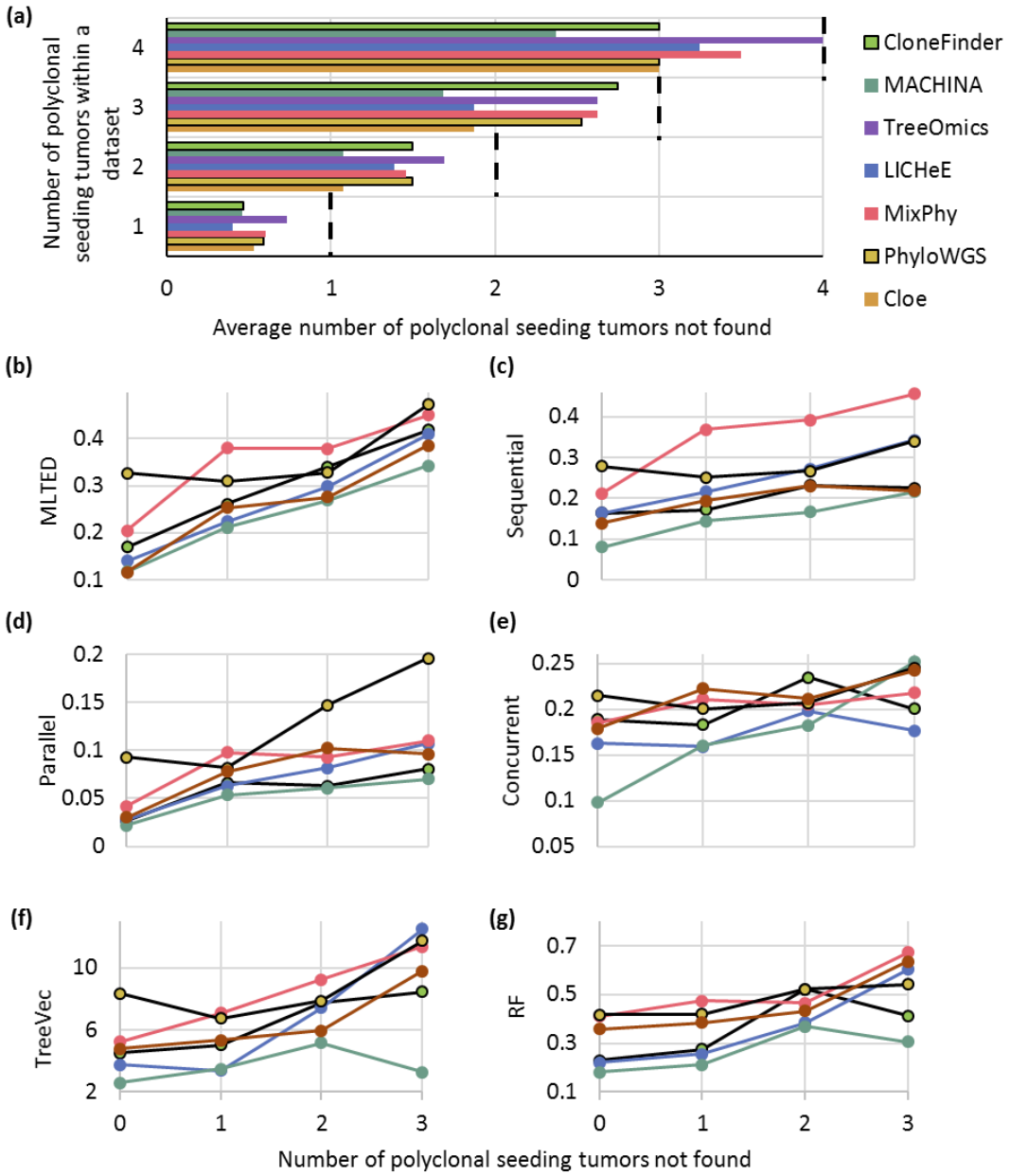

529

530 **Figure 7**: Accuracy of identifying different lineage clones within a tumor for the MA datasets. (**a**)
531 The average count of metastatic tumors with polyclonal seeding events that were not predicted.
532 (**b-g**) MLTED, error rates of ordering mutations, TreeVec, and RF distances. The x-axis for panels
533 **b-e** is the same as those in panels **f** and **g**. We excluded Cloe because its MLTED score was
534 very high, i.e., clone phylogenies were inaccurate.

bioRxiv preprint doi: https://doi.org/10.1101/697318; this version posted July 19, 2019. The copyright holder for this preprint (which was not certified by peer review) is the author/funder, who has granted bioRxiv a license to display the preprint in perpetuity. It is made available under aCC-BY-NC-ND 4.0 International license.

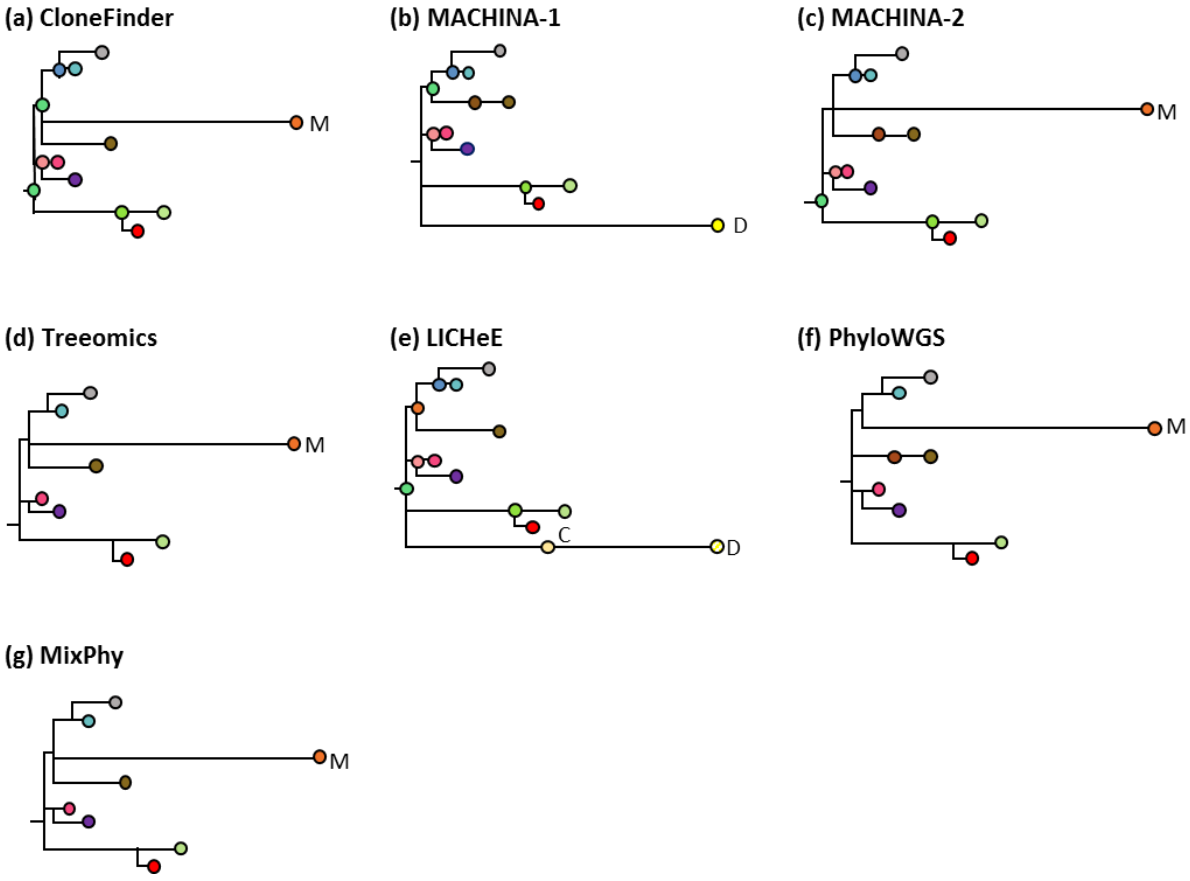

Figure 8. Clone phylogenies inferred by six methods (Cloe method was excluded due to error-prone) on an MA dataset. True clone phylogeny is given in **Figure 1g**. MACHINA produced two solutions (**b** and **c**). Inferred clones are annotated, and colors correspond to clones in **Figure 1g**. All the method produced either clone lineage M or lineage C/D, which were found in the M5 tumor (**Fig. 1h**). The first solution of MACHINA (**b**) produced clone D, and LICHeE produced clones C and D (**e**). The other methods produced clone M.

bioRxiv preprint doi: https://doi.org/10.1101/697318; this version posted July 19, 2019. The copyright holder for this preprint (which was not certified by peer review) is the author/funder, who has granted bioRxiv a license to display the preprint in perpetuity. It is made available under aCC-BY-NC-ND 4.0 International license.

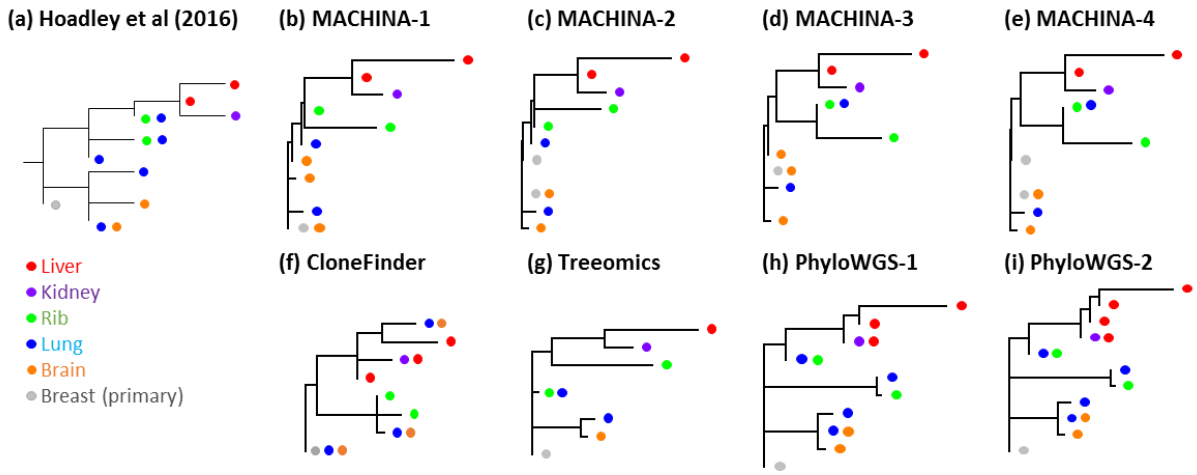

543

544 **Figure 9**: Empirical data analysis for the A7 dataset. The color of clones in the phylogeny
545 corresponds to the location of clones' samples. (**a**) Clone phylogeny reported by Hoadley et al.
546 (2016). (**b-i**) Inferred clone phylogenies by using (**b-e**) MACHINA, (**f**) CloneFInder, (**g**) Treeomics,
547 and (**h** and **i**) PhyloWGS. MACHINA and PhyloWGS produced more than one phylogeny.

548

549

bioRxiv preprint doi: https://doi.org/10.1101/697318; this version posted July 19, 2019. The copyright holder for this preprint (which was not certified by peer review) is the author/funder, who has granted bioRxiv a license to display the preprint in perpetuity. It is made available under aCC-BY-NC-ND 4.0 International license.

Abbreviations

SNV: single-nucleotide variant

VAF: variant allele frequency

CNV: copy number alteration

Declarations

Ethics approval and consent to participate

Not applicable.

Consent for publication

Not applicable.

Availability of data and material

The G7, G12, and P10 datasets are available on the website of the CloneFInder software (https://github.com/gstecher/CloneFinderAPI). The MA datasets and A7 dataset were obtained from the website of the MACHINA software (https://github.com/raphael-group/machina).

Competing interests

The authors declare that they have no competing interests.

Funding

This work was supported by National Institutes of Health to S.K. (LM012487) and S.M. (LM012758).

Authors' contributions

bioRxiv preprint doi: https://doi.org/10.1101/697318; this version posted July 19, 2019. The copyright holder for this preprint (which was not certified by peer review) is the author/funder, who has granted bioRxiv a license to display the preprint in perpetuity. It is made available under aCC-BY-NC-ND 4.0 International license.

SK conceived the project. SM and SK designed analyses. SM, TV, JD, TB, and JC performed the analyses. SK, SM, and TV wrote the manuscript. All authors read and approved the final manuscript.

Acknowledgments

We thank Drs. Antonia Chroni, Heather Rowe, Louise A Huuki, Zachary Hanson-Hart, and Viriya Keo for critical comments and technical support.

Additional files

Additional file 1: **Table S1 and Figures S1-S3**. Supplementary table and figures. (PDF)

References

1. Watson IR, Takahashi K, Futreal PA, Chin L: **Emerging patterns of somatic mutations in cancer**. *Nat Rev Genet* 2013, **14**(10):703-718.
2. Martincorena I, Campbell PJ: **Somatic mutation in cancer and normal cells**. *Science* 2015, **349**(6255):1483-1489.
3. Frank SA, Nowak MA: **Problems of somatic mutation and cancer**. *Bioessays* 2004, **26**(3):291-299.
4. Davis A, Gao R, Navin N: **Tumor evolution: Linear, branching, neutral or punctuated?** *Biochim Biophys Acta* 2017, **1867**(2):151-161.
5. McGranahan N, Swanton C: **Biological and therapeutic impact of intratumor heterogeneity in cancer evolution**. *Cancer Cell* 2015, **27**(1):15-26.
6. Gerlinger M, Rowan A, Horswell S, Larkin J, Endesfelder D, Gronroos E, Martinez P, Matthews N, Stewart A, Tarpey P *et al*: **Intratumor heterogeneity and branched evolution revealed by multiregion sequencing**. *N Engl J Med* 2012, **366**:883 - 892.
7. Marusyk A, Polyak K: **Tumor heterogeneity: causes and consequences**. *Biochim Biophys Acta* 2010, **1805**(1):105-117.
8. Dagogo-Jack I, Shaw AT: **Tumour heterogeneity and resistance to cancer therapies**. *Nat Rev Clin Oncol* 2018, **15**(2):81-94.
9. McGranahan N, Swanton C: **Clonal Heterogeneity and Tumor Evolution: Past, Present, and the Future**. *Cell* 2017, **168**(4):613-628.
10. Swanton C: **Intratumor heterogeneity: evolution through space and time**. *Cancer Res* 2012, **72**(19):4875-4882.
11. Naxerova K, Jain RK: **Using tumour phylogenetics to identify the roots of metastasis in humans**. *Nat Rev Clin Oncol* 2015, **12**(5):258-272.
12. Greaves M, Maley C: **Clonal evolution in cancer**. *Nature* 2012, **481**:306 - 313.
13. El-Kebir M, Satas G, Raphael BJ: **Inferring parsimonious migration histories for metastatic cancers**. *Nat Genet* 2018, **50**(5):718-726.

bioRxiv preprint doi: https://doi.org/10.1101/697318; this version posted July 19, 2019. The copyright holder for this preprint (which was not certified by peer review) is the author/funder, who has granted bioRxiv a license to display the preprint in perpetuity. It is made available under aCC-BY-NC-ND 4.0 International license.

14. Brown D, Smeets D, Szekely B, Larsimont D, Szasz AM, Adnet PY, Rothe F, Rouas G, Nagy ZI, Farago Z *et al*: **Phylogenetic analysis of metastatic progression in breast cancer using somatic mutations and copy number aberrations**. *Nat Commun* 2017, **8**:14944.
15. Zhao ZM, Zhao B, Bai Y, Iamarino A, Gaffney SG, Schlessinger J, Lifton RP, Rimm DL, Townsend JP: **Early and multiple origins of metastatic lineages within primary tumors**. *Proc Natl Acad Sci U S A* 2016, **113**(8):2140-2145.
16. Turajlic S, Xu H, Litchfield K, Rowan A, Chambers T, Lopez JI, Nicol D, O'Brien T, Larkin J, Horswell S *et al*: **Tracking Cancer Evolution Reveals Constrained Routes to Metastases: TRACERx Renal**. *Cell* 2018, **173**(3):581-594 e512.
17. Somarelli JA, Ware KE, Kostadinov R, Robinson JM, Amri H, Abu-Asab M, Fourie N, Diogo R, Swofford D, Townsend JP: **PhyloOncology: Understanding cancer through phylogenetic analysis**. *Biochim Biophys Acta Rev Cancer* 2017, **1867**(2):101-108.
18. Schwartz R, Schaffer AA: **The evolution of tumour phylogenetics: principles and practice**. *Nat Rev Genet* 2017, **18**(4):213-229.
19. Hong WS, Shpak M, Townsend JP: **Inferring the origin of metastases from cancer phylogenies**. *Cancer Res* 2015, **75**(19):4021-4025.
20. Macintyre G, Van Loo P, Corcoran NM, Wedge DC, Markowetz F, Hovens CM: **How subclonal modeling is changing the metastatic paradigm**. *Clin Cancer Res* 2017, **23**(3):630-635.
21. Kroigard AB, Larsen MJ, Brasch-Andersen C, Laenkholm AV, Knoop AS, Jensen JD, Bak M, Mollenhauer J, Thomassen M, Kruse TA: **Genomic Analyses of Breast Cancer Progression Reveal Distinct Routes of Metastasis Emergence**. *Sci Rep* 2017, **7**:43813.
22. Ullah I, Karthik GM, Alkodsi A, Kjallquist U, Stalhammar G, Lovrot J, Martinez NF, Lagergren J, Hautaniemi S, Hartman J *et al*: **Evolutionary history of metastatic breast cancer reveals minimal seeding from axillary lymph nodes**. *J Clin Invest* 2018, **128**(4):1355-1370.
23. Wang D, Niu X, Wang Z, Song CL, Huang Z, Chen KN, Duan J, Bai H, Xu J, Zhao J *et al*: **Multiregion Sequencing Reveals the Genetic Heterogeneity and Evolutionary History of Osteosarcoma and Matched Pulmonary Metastases**. *Cancer Res* 2019, **79**(1):7-20.
24. da Silva-Coelho P, Kroeze LI, Yoshida K, Koorenhof-Scheele TN, Knops R, van de Locht LT, de Graaf AO, Massop M, Sandmann S, Dugas M *et al*: **Clonal evolution in myelodysplastic syndromes**. *Nat Commun* 2017, **8**:15099.
25. Hunter KW, Amin R, Deasy S, Ha NH, Wakefield L: **Genetic insights into the morass of metastatic heterogeneity**. *Nat Rev Cancer* 2018, **18**(4):211-223.
26. Turajlic S, Xu H, Litchfield K, Rowan A, Horswell S, Chambers T, O'Brien T, Lopez JI, Watkins TBK, Nicol D *et al*: **Deterministic Evolutionary Trajectories Influence Primary Tumor Growth: TRACERx Renal**. *Cell* 2018, **173**(3):595-610 e511.
27. Nik-Zainal S, Van Loo P, Wedge DC, Alexandrov LB, Greenman CD, Lau KW, Raine K, Jones D, Marshall J, Ramakrishna M *et al*: **The life history of 21 breast cancers**. *Cell* 2012, **149**(5):994-1007.
28. Cooper CS, Eeles R, Wedge DC, Van Loo P, Gundem G, Alexandrov LB, Kremeyer B, Butler A, Lynch AG, Camacho N *et al*: **Analysis of the genetic phylogeny of multifocal prostate cancer identifies multiple independent clonal expansions in neoplastic and morphologically normal prostate tissue**. *Nat Genet* 2015, **47**(4):367-372.

bioRxiv preprint doi: https://doi.org/10.1101/697318; this version posted July 19, 2019. The copyright holder for this preprint (which was not certified by peer review) is the author/funder, who has granted bioRxiv a license to display the preprint in perpetuity. It is made available under aCC-BY-NC-ND 4.0 International license.

29. Stachler MD, Taylor-Weiner A, Peng S, McKenna A, Agoston AT, Odze RD, Davison JM, Nason KS, Loda M, Leshchiner I *et al*: **Paired exome analysis of Barrett's esophagus and adenocarcinoma**. *Nat Genet* 2015, **47**(9):1047-1055.
30. Hoadley KA, Siegel MB, Kanchi KL, Miller CA, Ding L, Zhao W, He X, Parker JS, Wendl MC, Fulton RS *et al*: **Tumor Evolution in Two Patients with Basal-like Breast Cancer: A Retrospective Genomics Study of Multiple Metastases**. *PLoS Med* 2016, **13**(12):e1002174.
31. Gawad C, Koh W, Quake SR: **Single-cell genome sequencing: current state of the science**. *Nat Rev Genet* 2016, **17**(3):175-188.
32. Navin NE: **The first five years of single-cell cancer genomics and beyond**. *Genome Res* 2015, **25**(10):1499-1507.
33. Vandin F: **Computational methods for characterizing cancer mutational heterogeneity**. *Front Genet* 2017, **8**:83.
34. Popic V, Salari R, Hajirasouliha I, Kashef-Haghighi D, West RB, Batzoglou S: **Fast and scalable inference of multi-sample cancer lineages**. *Genome Biol* 2015, **16**(1):91.
35. Miura S, Gomez K, Murillo O, Huuki LA, Vu T, Buturla T, Kumar S: **Predicting clone genotypes from tumor bulk sequencing of multiple samples**. *Bioinformatics* 2018, **34**(23):4017-4026.
36. Reiter JG, Makohon-Moore AP, Gerold JM, Bozic I, Chatterjee K, Iacobuzio-Donahue CA, Vogelstein B, Nowak MA: **Reconstructing metastatic seeding patterns of human cancers**. *Nat Commun* 2017, **8**:14114.
37. Deshwar AG, Vembu S, Yung CK, Jang GH, Stein L, Morris Q: **PhyloWGS: reconstructing subclonal composition and evolution from whole-genome sequencing of tumors**. *Genome Biol* 2015, **16**:35.
38. Hujdurovic A, Kacar U, Milanic M, Ries B, Tomescu AI: **Complexity and Algorithms for Finding a Perfect Phylogeny from Mixed Tumor Samples**. *IEEE/ACM Trans Comput Biol Bioinform* 2018, **15**(1):96-108.
39. Marass FM, Florent; Yuan, Ke; Rosenfeld, Nitzan; Markowetz, Florian: **A phylogenetic latent feature model for clonal deconvolution**. *Ann Appl Stat* 2016, **10**(4):2377--2404.
40. Um SW, Joung JG, Lee H, Kim H, Kim KT, Park J, Hayes DN, Park WY: **Molecular Evolution Patterns in Metastatic Lymph Nodes Reflect the Differential Treatment Response of Advanced Primary Lung Cancer**. *Cancer Res* 2016, **76**(22):6568-6576.
41. Gundem G, Van Loo P, Kremeyer B, Alexandrov LB, Tubio JM, Papaemmanuil E, Brewer DS, Kallio HM, Hognas G, Annala M *et al*: **The evolutionary history of lethal metastatic prostate cancer**. *Nature* 2015, **520**(7547):353-357.
42. Yang H, Lu B, Lai LH, Lim AH, Alvarez JJS, Zhai W: **PSiTE: a Phylogeny guided Simulator for Tumor Evolution**. *Bioinformatics* 2019.
43. Davis A, Navin NE: **Computing tumor trees from single cells**. *Genome Biol* 2016, **17**(1):113.
44. Gerlinger M, Horswell S, Larkin J, Rowan AJ, Salm MP, Varela I, Fisher R, McGranahan N, Matthews N, Santos CR *et al*: **Genomic architecture and evolution of clear cell renal cell carcinomas defined by multiregion sequencing**. *Nat Genet* 2014, **46**(3):225-233.
45. Ling S, Hu Z, Yang Z, Yang F, Li Y, Lin P, Chen K, Dong L, Cao L, Tao Y *et al*: **Extremely high genetic diversity in a single tumor points to prevalence of non-Darwinian cell evolution**. *Proc Natl Acad Sci U S A* 2015, **112**(47):E6496-6505.
46. Malikic S, McPherson AW, Donmez N, Sahinalp CS: **Clonality inference in multiple tumor samples using phylogeny**. *Bioinformatics* 2015, **31**(9):1349-1356.

bioRxiv preprint doi: https://doi.org/10.1101/697318; this version posted July 19, 2019. The copyright holder for this preprint (which was not certified by peer review) is the author/funder, who has granted bioRxiv a license to display the preprint in perpetuity. It is made available under aCC-BY-NC-ND 4.0 International license.

47. Sengupta S, Wang J, Lee J, Muller P, Gulukota K, Banerjee A, Ji Y: **Bayclone: Bayesian nonparametric inference of tumor subclones using NGS data**. *Pac Symp Biocomput* 2015:467-478.
48. Zare H, Wang J, Hu A, Weber K, Smith J, Nickerson D, Song C, Witten D, Blau CA, Noble WS: **Inferring clonal composition from multiple sections of a breast cancer**. *PLoS Comput Biol* 2014, **10**(7):e1003703.
49. Jiang Y, Qiu Y, Minn AJ, Zhang NR: **Assessing intratumor heterogeneity and tracking longitudinal and spatial clonal evolutionary history by next-generation sequencing**. *Proc Natl Acad Sci U S A* 2016, **113**(37):E5528-5537.
50. Fischer A, Vazquez-Garcia I, Illingworth CJ, Mustonen V: **High-definition reconstruction of clonal composition in cancer**. *Cell Rep* 2014, **7**(5):1740-1752.
51. El-Kebir M, Oesper L, Acheson-Field H, Raphael BJ: **Reconstruction of clonal trees and tumor composition from multi-sample sequencing data**. *Bioinformatics* 2015, **31**(12):i62-i70.
52. Strino F, Parisi F, Micsinai M, Kluger Y: **TrAp: a tree approach for fingerprinting subclonal tumor composition**. *Nucleic Acids Res* 2013.
53. Roth A, Khattra J, Yap D, Wan A, Laks E, Biele J, Ha G, Aparicio S, Bouchard-Cote A, Shah SP: **PyClone: statistical inference of clonal population structure in cancer**. *Nat Methods* 2014, **11**(4):396-398.
54. Miller CA, White BS, Dees ND, Griffith M, Welch JS, Griffith OL, Vij R, Tomasson MH, Graubert TA, Walter MJ *et al*: **SciClone: Inferring Clonal Architecture and Tracking the Spatial and Temporal Patterns of Tumor Evolution**. *PLoS Comput Biol* 2014, **10**(8):e1003665.
55. Jahn K, Kuipers J, Beerenwinkel N: **Tree inference for single-cell data**. *Genome Biol* 2016, **17**:86.
56. Miura S, Huuki LA, Buturla T, Vu T, Gomez K, Kumar S: **Computational enhancement of single-cell sequences for inferring tumor evolution**. *Bioinformatics* 2018, **34**(17):i917-i926.
57. Kuhn HWT, A. W.: **Nonlinear programming**. In: *Proceedings of the Second Berkeley Symposium on Mathematical Statistics and Probability, 1950.* 1951: 481--492.
58. Karpov NM, S.; Rahman, K.; Sahinalp, S.C.: **A Multi-labeled Tree Edit Distance for Comparing "Clonal Trees" of Tumor Progression**. In: *18th International Workshop on Algorithms in Bioinformatics (WABI 2018). Volume 113*, edn. Edited by Parida LU, E. Dagstuhl, Germany: Schloss Dagstuhl--Leibniz-Zentrum fuer Informatik; 2018.
59. Kendall M, Eldholm V, Colijn C: **Comparing phylogenetic trees according to tip label categories**. *bioRxiv* 2018:251710.
60. Nei M, Kumar S: **Molecular evolution and phylogenetics**. Oxford ; New York: Oxford University Press; 2000.
61. Kumar S, Stecher G, Peterson D, Tamura K: **MEGA-CC: Computing Core of Molecular Evolutionary Genetics Analysis program for automated and iterative data analysis**. *Bioinformatics* 2012, **28**:2685-2686
62. Kuhner MK, Yamato J: **Practical performance of tree comparison metrics**. *Syst Biol* 2015, **64**(2):205-214.
63. Kendall M, Colijn C: **Mapping Phylogenetic Trees to Reveal Distinct Patterns of Evolution**. *Mol Biol Evol* 2016, **33**(10):2735-2743.
64. Jombart T, Kendall M, Almagro-Garcia J, Colijn C: **treespace: Statistical exploration of landscapes of phylogenetic trees**. *Mol Ecol Resour* 2017, **17**(6):1385-1392.
65. Robinson DF, Foulds LR: **Comparison of Phylogenetic Trees**. *Mathematical Biosciences* 1981, **53**(1-2):131-147.

bioRxiv preprint doi: https://doi.org/10.1101/697318; this version posted July 19, 2019. The copyright holder for this preprint (which was not certified by peer review) is the author/funder, who has granted bioRxiv a license to display the preprint in perpetuity. It is made available under aCC-BY-NC-ND 4.0 International license.

747 66. Wen D, Yu Y, Zhu J, Nakhleh L: **Inferring Phylogenetic Networks Using PhyloNet**. *Syst*
748 *Biol* 2018, **67**(4):735-740.

749